Research Article

Yuhong Qian, Yiting Wang, and Li Wang*

Preparation of cuprous oxide-supported silver-modified reduced graphene oxide nanocomposites for non-enzymatic electrochemical sensor

https://doi.org/10.1515/revac-2022-0045 received June 12, 2022; accepted August 18, 2022

Abstract: We constructed a non-enzymatic H_2O_2 sensor based on cuprous oxide-supported silver-modified reduced graphene oxide nanocomposites. It was found that the sensor exhibited good performances for sensing H_2O_2 with a detection limit of $0.34\,\mu\text{M}$ and a wide detection range of $1\text{--}310\,\mu\text{M}$. The combination of graphene with silver and cuprous oxide improved the sensor's sensitivity for detecting H_2O_2 , with good repeatability, selectivity, and stability. The synthesis method of this nanocomposite provides a new idea for the green preparation of graphene-based nanocomposites and a new method for the construction of a new electrochemical sensor platform.

Keywords: cuprous oxide, silver, reduced graphene oxide, sensor

1 Introduction

Rapid and sensitive methods for detecting H_2O_2 have broad application prospects in the fields of food, medicine, chemical industry, and environmental protection and have attracted much attention in recent years [1–3]. Among many methods for detecting H_2O_2 , the electrochemical method is considered promising because of its high sensitivity and simple operation [4]. With the development of materials science and nanotechnology, nanomaterials with mimetic enzymatic activities have been widely used for the modification of chemical electrodes

to fabricate non-enzymatic sensors and biosensors. It has been reported that some nanomaterials such as two-dimensional (2D) materials, metallic nanoparticles, metal oxides, and others reveal potential enzymatic activity that is similar to natural enzymes, and therefore, could catalyze the oxidization and reduction of H_2O_2 that could be done by natural enzymes previously [5–8].

Graphene is a material with sp² hybrid connected carbon atoms closely packed into a single-layer 2D cellular lattice structure. Due to the excellent optical, electrical, and mechanical properties of graphene, graphene and graphene-based hybrid materials have been widely applied to materials science, micro-nano processing, energy, biomedicine, and drug delivery [9-11]. Graphene is considered to be a revolutionary material for the future. Previously, graphene-based non-enzymatic electrochemical sensors for high-performance detection of H2O2 and glucose have been reported [12]. In some cases, to improve the sensing performance, other metallic and metal oxide nanoparticles have been incorporated with graphene to form 2D nanocomposites, which exhibited synergistic effects for enhancing the electrochemical sensing efficiency [13-15].

Silver (Ag) nanomaterials have been widely applied in the fields of surface-enhanced Raman scattering (SERS), transparent conductive films, catalysts, sensors, and antibacterial sterilization due to their unique electrical, optical, thermal, catalytic, and elastic properties [16–20]. Cuprous oxide (Cu₂O) is a low-cost, environment-friendly p-type semiconductor with a narrow band gap [21], and therefore Cu₂O-based materials have been used widely in catalysis, sensors, solar cells, lithium-ion batteries, and water splitting [22–25]. The combination of Ag with Cu₂O has attracted strong attention, and Ag-Cu₂O nanocomposites for different purposes have been synthesized [26–28]. For instance, Luo et al. used Ag nanoparticles to decorate the surface of the prepared Cu₂O cubes. The Cu₂O/Ag heterostructures within the cellulose nanofibril

^{*} Corresponding author: Li Wang, College of Chemistry, Jilin Normal University, Siping, 136000, China, e-mail: liwang@jlnu.edu.cn Yuhong Qian, Yiting Wang: College of Chemistry, Jilin Normal University, Siping, 136000, China

network were employed as an SERS substrate for efficient sensing of methylene blue [29]. Hu and coworkers prepared a series of Cu₂O/Ag heterojunctions using a simple microwave-assisted green route. The study of antibacterial behavior against Escherichia coli and Staphylococcus aureus indicated that the heterojunction exhibited much better antibacterial performance than the pristine Cu₂O due to the synergistic effect of Cu₂O and Ag [30]. The combination of graphene with Ag and Cu₂O may lead to unique nanomaterials with novel functions [20,31,32]. For example, Sharma et al. synthesized ternary nanocomposites composed of Ag-Cu₂O and reduced graphene oxide (rGO) using Benedict's solution and glucose solution without any toxic reagent, surfactant, or special treatment [33]. The resulting Ag-Cu₂O/rGO nanocomposites exhibited good photocatalytic performance for the photodegradation of methyl orange.

In this work, we used the catalytic activity of Ag nanoparticles on $\rm H_2O_2$ to modify rGO and then combined the products with $\rm Cu_2O$ to form $\rm Cu_2O/Ag$ -rGO nanocomposites. It was found that the nanocomposites exhibited good electrocatalytic properties for $\rm H_2O_2$. The results showed that our method was simple and green, and the sensor based on the $\rm Cu_2O/Ag$ -rGO nanocomposites had the advantages of high sensitivity, high selectivity, and a wide detection range. This method provides not only a highly selective and sensitive electrochemical detection platform for the detection of $\rm H_2O_2$, but also a new idea for the application of graphene-based metal nanocomposites in the field of electrochemical biosensors.

2 Experimental sections

2.1 Reagents and materials

Ethanol (>99.9%, analytically pure), polyvinylpyrrolidone (PVP, K30, $M_{\rm w}=30,000$ –40,000), hydrogen peroxide (H₂O₂, 30 wt%), silver nitrate, copper nitrate, sodium citrate dihydrate (1 wt%), hydrazine hydrate (40%, analytically pure), concentrated nitric acid (68 wt%), glucose (analytically pure), and ascorbic acid (AA, >99.7%, analytically pure) were purchased from Beijing Chemical Plant. Monolayer graphene oxide (GO) aqueous dispersion (10 mg·g⁻¹) was purchased from Hangzhou Gaosen Technology Co., Ltd. Dopamine hydrochloride (98%, analytically pure) was purchased from Aladdin Reagent Co., Ltd., and uric acid (UA, analytically pure) was purchased from Sigma Aldrich Chemical Reagent Co., Ltd. All reagents

were used directly without purification. Ultrapure water was used in the experiment.

2.2 Preparation of Cu₂O/Ag-rGO nanocomposites

2.2.1 Preparation of the Ag-rGO composite

After ultrasonic treatment of $0.1\,\mathrm{mg\cdot mL^{-1}}$ of monolayer GO solution, $30\,\mathrm{mL}$ of the treated solution was taken and poured into a three-port flask, and then water was added up to $200\,\mathrm{mL}$. Next, $36\,\mathrm{mg}$ of silver nitrate was added to the three-port flask and heated until the solution boiled. Then, $4\,\mathrm{mL}$ of sodium citrate solution was quickly added and stirred. Finally, the temperature was adjusted to $85^{\circ}\mathrm{C}$ and heated for $40\,\mathrm{min}$ to obtain the Ag-rGO composite structure.

2.2.2 Preparation of the Cu₂O/Ag-rGO composite

One gram of PVP was added to 50 mL of 0.04 M copper nitrate solution and stirred until PVP was fully dissolved. Then, 20 mL of the prepared Ag-rGO solution was added to this solution. Next, 68 μL of hydrazine hydrate was added to this solution and stirred. The obtained product was centrifuged and washed with water.

2.3 Instruments

The morphology of the obtained nanocomposites was investigated by an S-4800 scanning electron microscope (SEM) and a TECNAI G2 high-resolution transmission electron microscope (TEM). The crystalline nature of the nanostructures was analyzed using a Rigaku D/max 2500 V X-ray diffractometer. X-ray photoelectron spectroscopy (XPS) analyses were carried out on an Escalab-MkII energy spectrometer.

2.4 Detection of H₂O₂

 $\rm H_2O_2$ aqueous solutions with different concentrations were prepared by diluting $\rm H_2O_2$ in a gradient. All electrochemical properties of the samples were tested by a CHI 760e electrochemical analyzer (Shanghai Chenhua

Instrument Co., Ltd.) with the conventional three-electrode system. Saturated calomel electrode was used as the reference electrode, platinum wire as the counter electrode, and modified glassy carbon electrode (GCE) as the working electrode. The 3 mm diameter GCE was polished with alumina slurry, and then ultrasonically washed in water and ethanol for 5 min. When preparing the H₂O₂ sensor, 4 µL of Cu₂O/Ag-rGO solution was dropped on the clean GCE surface and dried in the air. In the control experiment, 4 μL of 1 mg·mL⁻¹ rGO solution was dropped on the bare GCE and dried as the working electrode. In the selective test, 5 µL of glucose, AA, UA, and dopamine (DA) were used as control. The current change in the system was investigated under the same experimental conditions as those for H₂O₂. Before the experiment, N₂ was pumped into the 0.1 M phosphate-buffered saline (PBS) solution (pH = 7.0) to remove the oxygen in the buffer and N2 was used in the whole electrochemical measurements.

Results and discussion

3.1 Characterizations of Cu₂O/Ag-rGO nanocomposites

The morphology and crystal structure of Cu₂O/Ag-rGO were characterized by SEM and TEM, as shown in Figure 1. SEM images show that Cu₂O/Ag nanoparticles are spherical in shape with the size of about 50-80 nm and the surface of the particles is rough (Figure 1a and b). To further confirm their micro-configuration and geometrical structure, the morphologies of the as-prepared Cu₂O/Ag nanocomposites were further analyzed by TEM (Figure 1c and d). It can be seen from Figure 1c that most Cu₂O/Ag nanoparticles are supported on rGO nanosheets. The Ag nanoparticles are evenly encapsulated by the rough Cu₂O layer. The evident contrast in the brightness between the dark cores and bright shells indicates the formation of core-shell architecture. Two distinct crystal

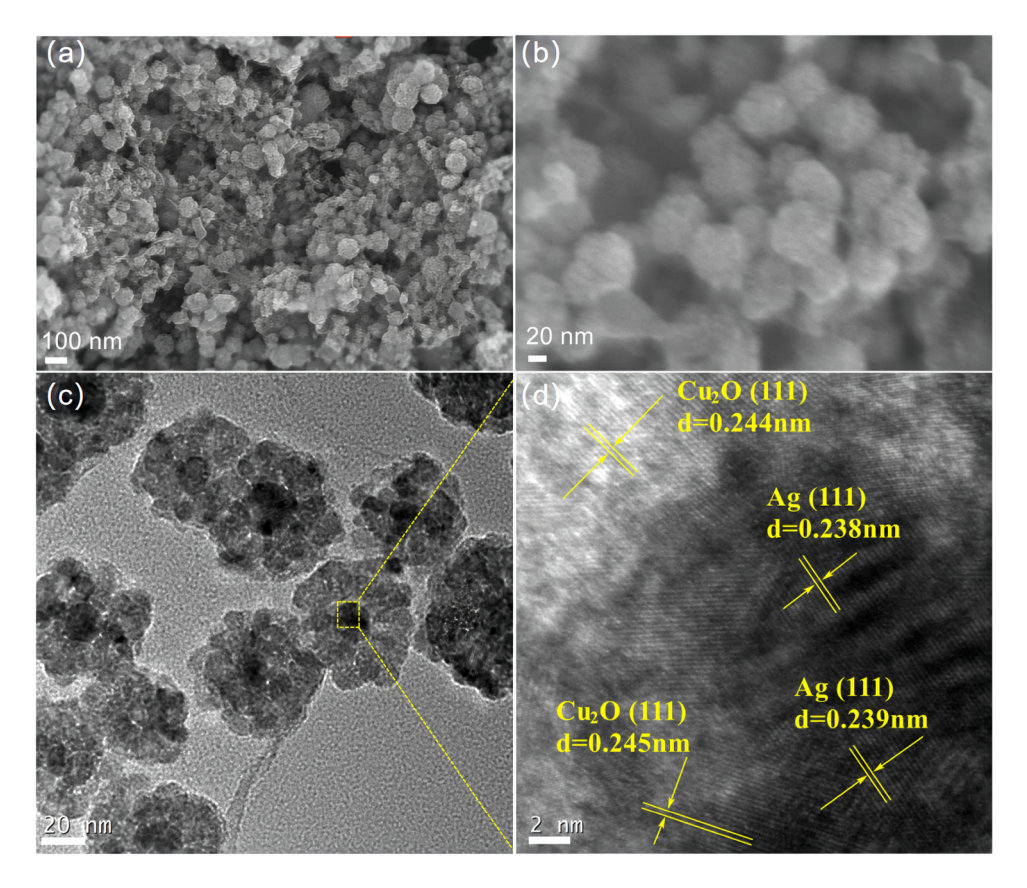


Figure 1: (a and b) SEM and (c and d) TEM images of Cu₂O/Ag-rGO nanocomposites.

structures can be observed in Figure 1d. High-resolution transmission electron microscopy shows that the fringe spacing of 0.244 nm is ascribed to (111) facet of Cu_2O nanoparticles, indicating that the exposed crystal facet of Cu_2O nanocrystals is (111) crystal facets. The fringe spacing of 0.238 nm corresponds to the (111) crystal planes of Ag nanoparticles [31].

XRD diffraction pattern shows that the main diffraction peaks of $\text{Cu}_2\text{O}/\text{Ag}\text{-rGO}$ in the range of $10\text{--}90^\circ$ are consistent with the previous reports [34], as shown in Figure 2. The strong intensity of the diffraction peaks indicates that the synthesized $\text{Cu}_2\text{O}/\text{Ag}\text{-rGO}$ nanocomposites have a well-ordered structure. The results prove the formation of the ternary heterojunction structure of $\text{Cu}_2\text{O}/\text{Ag}\text{-rGO}$. No other impurities are found in the figure, which demonstrates that the synthesized $\text{Cu}_2\text{O}/\text{Ag}\text{-rGO}$ nanocomposite is relatively pure.

The chemical composition and valence distribution of Cu₂O/Ag-rGO nanocomposites were characterized by XPS, as shown in Figure 3. C 1s, O 1s, Ag 3d, and Cu 2p in the full spectrum prove the existence of C, O, Ag, and Cu elements, respectively (Figure 3a). In Figure 3b, the binding energy peaks at 374.15 and 368.15 eV correspond to Ag 3d3/2 and Ag 3d5/2, respectively [35,36]. The binding energy peaks at 288.1, 285.95, 284.8, and 284.3 eV in the C 1s spectrum indicate that the structure contains C=O, C-O, C-C, and C=C [37], as shown in Figure 3c. In Figure 3d, the binding energy peaks at 532.95, 531.45, and 530.25 eV in the O 1s spectrum indicate that the structure contains C=O, C-OH, and Cu-O [38]. In Figure 3e, the binding energy peaks at 952.1 and 932.3 eV correspond to Cu 2p1/2 and Cu 2p3/2, respectively

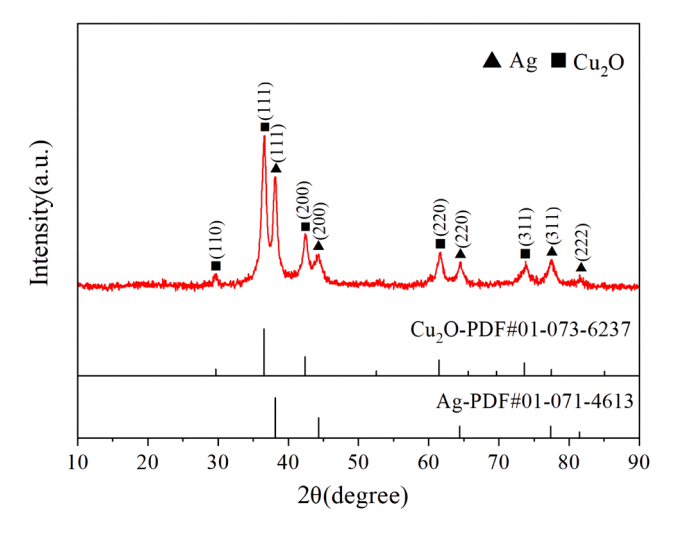


Figure 2: XRD diffraction patterns of Cu₂O/Ag-rGO nanocomposites.

[39]. The results prove the formation of Cu₂O/Ag-rGO nanocomposites.

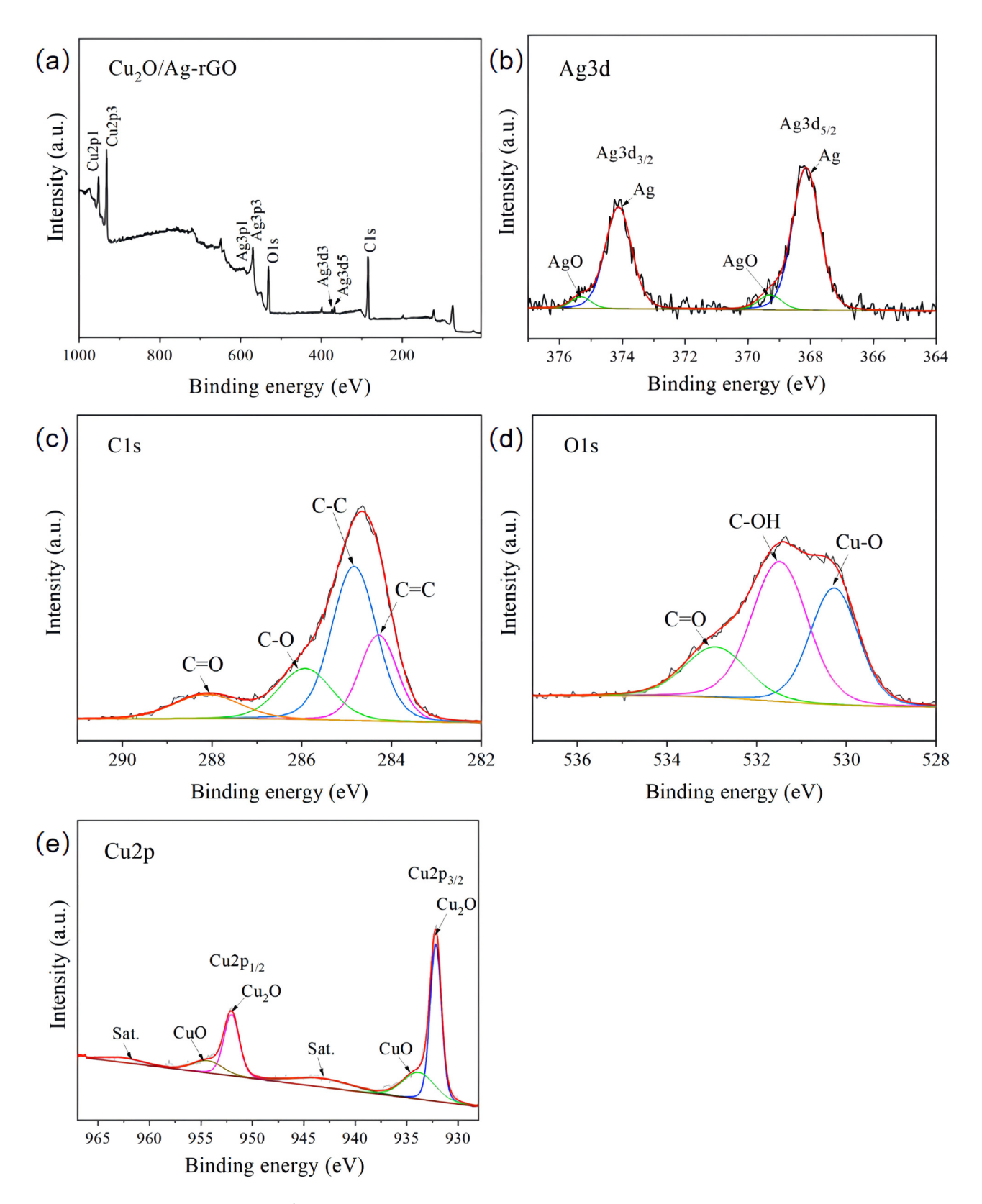
3.2 Optimization of H₂O₂ catalytic conditions

In order to explore the optimal conditions for the obtained $\text{Cu}_2\text{O}/\text{Ag-rGO}$ nanocomposites to catalyze H_2O_2 , control experiments were carried out. The catalytic performance of the nanocomposites was adjusted by controlling the amount of $\text{Cu}(\text{NO}_3)_2$ added into the reaction. Under the working potential of -0.4 V, H_2O_2 with different concentrations was added slowly into the working system to observe the current response. It can be seen from Figure 4 that the nanocomposites prepared with the addition of 0.04 M $\text{Cu}(\text{NO}_3)_2$ have the best catalytic effect on H_2O_2 .

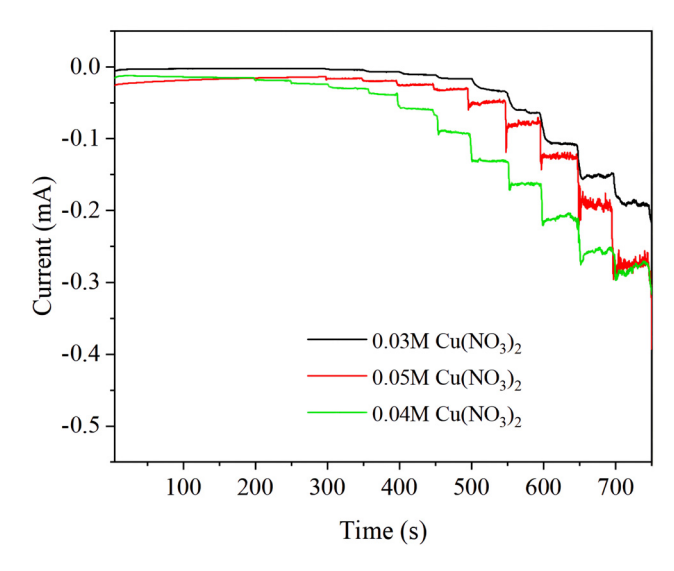
To prove that the prepared nanocomposites have good electrocatalytic activity, the catalytic behaviors of unmodified GCE, rGO-modified GCE, and the Cu₂O/Ag-rGO nanocomposite-modified GCE for H₂O₂ were compared, as shown in Figure 5. It can be seen that the unmodified GCE has no obvious oxidation-reduction process after adding 10 µM H₂O₂, while the diffusion current of GCE increased after rGO modification. In contrast, the current of the GCE modified by Cu₂O/Ag-rGO nanocomposites is significantly increased, indicating that the nanocomposites have reduced H₂O₂ on the electrode surface and form an amplified current signal. These results show that the Cu₂O/Ag-rGO nanocomposites have obvious electrocatalytic reduction activity for H₂O₂. The introduction of Cu₂O makes the local energy level in the nanocomposite change correspondingly, which is conducive to the transfer of electrons. The synergistic effect between Cu₂O and Ag could enhance the electrical conductivity of the electrode. Additionally, Cu₂O/Ag nanoparticles can disperse rGO and make it difficult to agglomerate, which increases the active surface areas of the modified electrode.

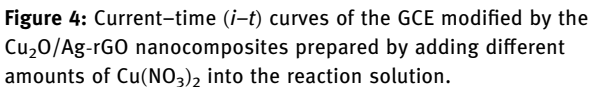
3.3 Sensitivity analysis of the detection system

Figure 6a shows a typical i-t curve with the Cu₂O/Ag-rGO nanocomposite-modified GCE on successive additions of H₂O₂ into the 0.1 M of PBS solution. It is clear that the addition of 1 μ M H₂O₂ causes a rapid and stable current response as a result of the reduction of H₂O₂. The



 $\textbf{Figure 3:} (a) \text{ XPS full spectrum of } \text{Cu}_2\text{O}/\text{Ag-rGO nanocomposites. High-resolution XPS spectra of (b) Ag 3d, (c) C 1s, (d) O 1s, and (e) Cu 2p. \\$





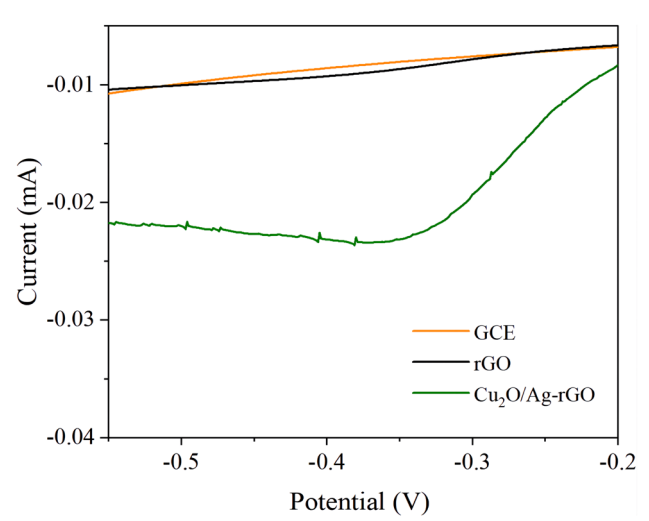


Figure 5: Cyclic voltammograms of bare GCE, rGO modified GCE, and Cu_2O/Ag -rGO nanocomposite-modified GCE toward the detection of H_2O_2 .

corresponding calibration of the i-t data indicates a regular response toward $\rm H_2O_2$ with a linear detection range from 1 to 310 μ M (Figure 6b). According to the linear fit, it can be concluded that the linear regression equation is I (mA) = -0.001c (μ M) -0.036. The calculated detection limit of this sensor is $0.34 \,\mu$ M (S/N = 3).

The selectivity and anti-interference of this electrochemical sensor were evaluated by adding glucose, AA, UA, and DA. Figure 7a shows that no interference is observed in the measured potential. Therefore, it can be concluded that this sensor has good anti-interference ability and high selectivity. The reuse stability of $\text{Cu}_2\text{O}/\text{Ag-rGO}$ nanocomposite-modified GCE was further investigated. Figure 7b shows that the fabricated sensor can be reused at least five times. The long-term stability of $\text{Cu}_2\text{O}/\text{Ag-rGO}$ nanocomposite-modified GCE within 14 days was studied. The prepared electrodes were stored in a refrigerator at 4°C and measured once after 1, 2, 3, 7, and 14 days. Figure 7c shows that after 14 days, the reduction current response of $10\,\mu\text{M}$ H₂O₂ remains at 85.4% of the initial value, revealing that the sensor based on $\text{Cu}_2\text{O}/\text{Ag-rGO}$ nanocomposites has acceptable stability.

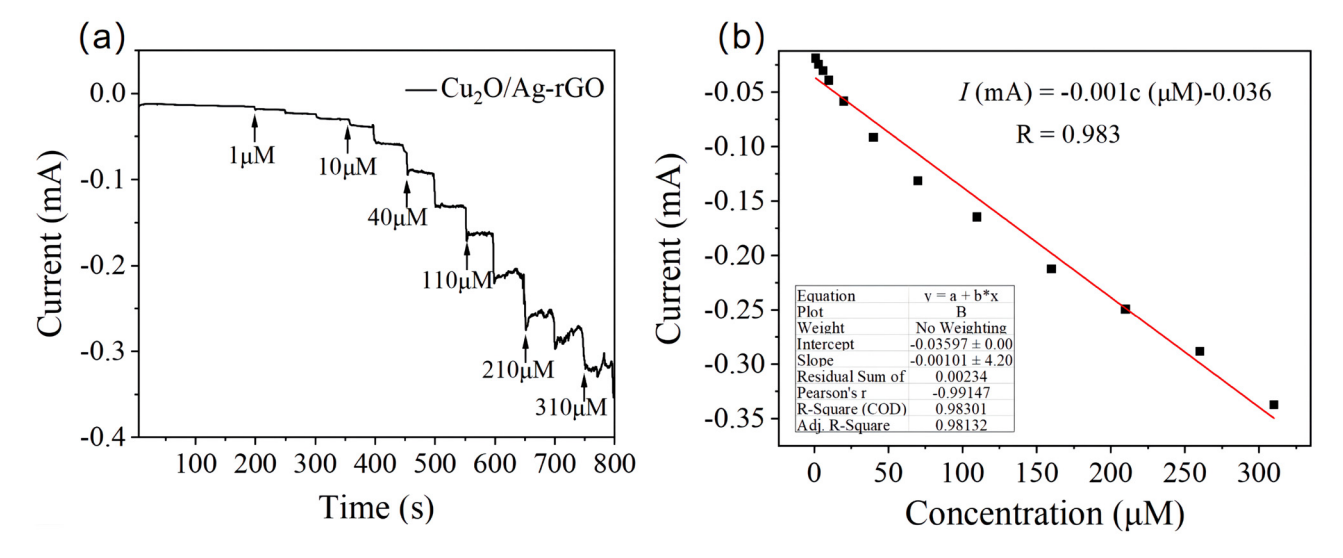


Figure 6: Electrochemical sensing H_2O_2 : (a) i-t response of the Cu_2O/Ag -rGO nanocomposite-modified GCE by adding H_2O_2 with various concentrations, and (b) corresponding calibration line of current against the concentration of H_2O_2 .

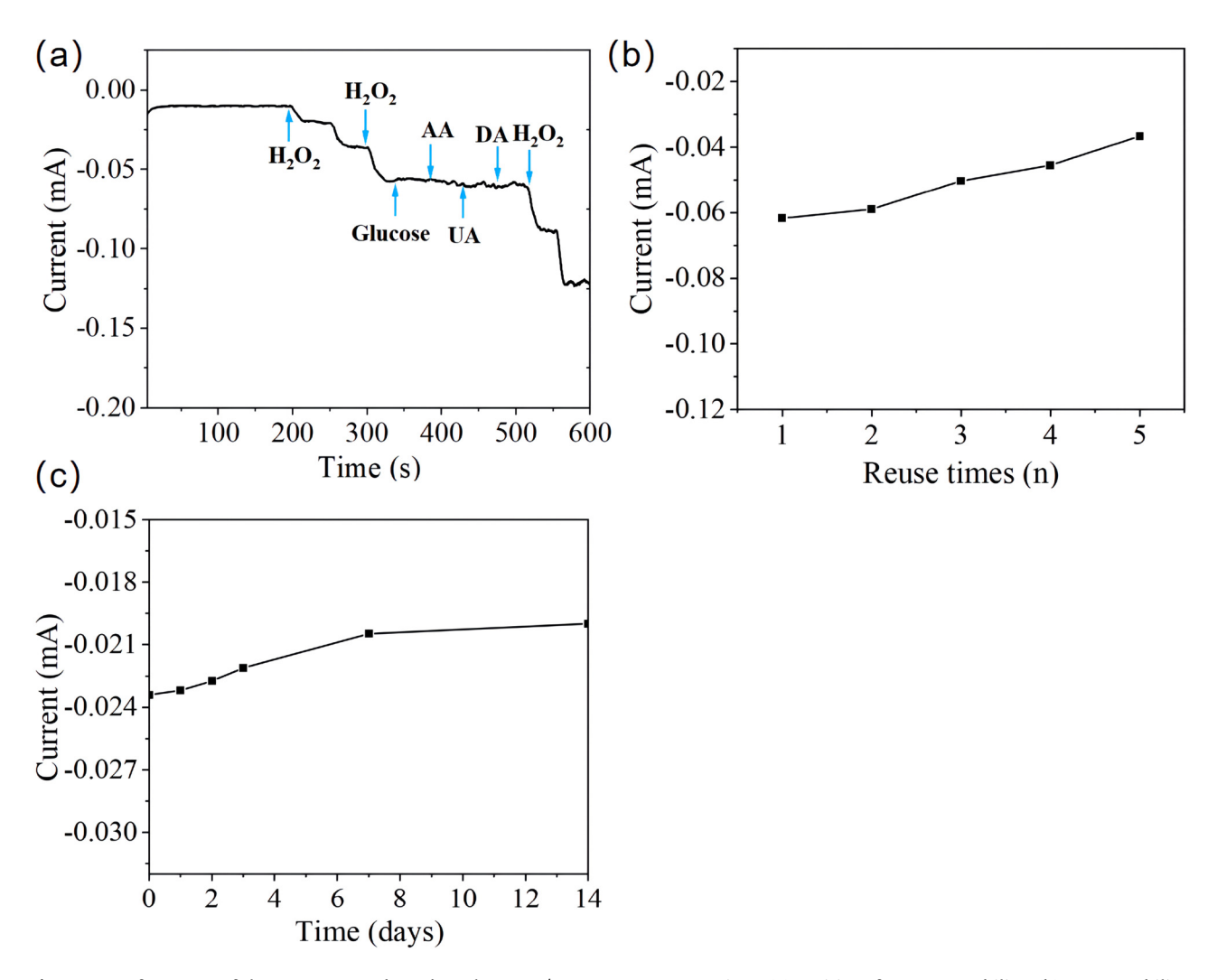


Figure 7: Performance of the H_2O_2 sensor based on the Cu_2O/Ag -rGO nanocomposites: (a) anti-interference capability, (b) reuse stability, and (c) long-term stability.

4 Conclusions

In this work, we proposed a method based on the Cu_2O/Ag -rGO nanocomposites to construct a nonenzymatic H_2O_2 sensor with high sensitivity and selectivity. We studied and analyzed the electrochemical performance of the sensor based on the Cu_2O/Ag -rGO nanocomposites. The sensor exhibits a wide detection range of 1–310 μ M and a relatively low detection limit of 0.34 μ M. Compared with the traditional method, our method has the advantages of being a simple experimental process, using a simple instrument, and being environmentally friendly. Furthermore, this method provides a new idea for the construction of a fast, sensitive, economical, and highly selective non-enzymatic H_2O_2 sensor, which has theoretical and practical significance.

Funding information: This research was financially supported by the National Natural Science Foundation of China (Grant No. 21505049).

Author contributions: Yuhong Qian: writing – original draft, methodology, data analysis; Yiting Wang: formal analysis; Li Wang: writing – original draft, writing – review and editing, project administration.

Conflict of interest: The authors state no conflict of interest.

References

 Zhang M, Yang N, Liu Y, Tang J. Synthesis of catalase-inorganic hybrid nanoflowers via sonication for colorimetric

- detection of hydrogen peroxide. Enzyme Microb Technol. 2019;128:22-5.
- [2] Abdelhamid HN, Sharmoukh W. Intrinsic catalase-mimicking MOFzyme for sensitive detection of hydrogen peroxide and ferric ions. Microchem J. 2021;163:105873.
- [3] Zhang M, Chen M, Liu Y, Wang Y, Tang J. Catalase-inorganic hybrid microflowers modified glassy carbon electrode for amperometric detection of hydrogen peroxide. Mater Lett. 2019;243:9–12.
- [4] Park J, Kim JW, Kim H, Yoon W. An electrochemical hydrogen peroxide sensor for applications in nuclear industry. Nucl Eng Technol. 2021;53:142-7.
- [5] Tian Q, Jing L, Chen Y, Su P, Tang C, Wang G, et al. Micelle-templating interfacial self-assembly of two-dimensional mesoporous nanosheets for sustainable H₂O₂ electrosynthesis. Sustain Mater Technol. 2022;e00398. https://www.sciencedirect.com/science/article/pii/S2214993722000124.
- [6] Gholami M, Koivisto B. A flexible and highly selective nonenzymatic H₂O₂ sensor based on silver nanoparticles embedded into Nafion. Appl Surf Sci. 2019;467:112–8.
- [7] Zhang W, Chen X, Zhao X, Yin M, Feng L, Wang H, et al. Simultaneous nitrogen doping and Cu₂O oxidization by one-step plasma treatment toward nitrogen-doped Cu₂O@CuO heterostructure: An efficient photocatalyst for H₂O₂ evolution under visible light. Appl Surf Sci. 2020;527:146908.
- [8] Li J, Jiang J, Xua Z, Liu M, Tang S, Yang C, et al. Facile synthesis of Ag@Cu₂O heterogeneous nanocrystals decorated N-doped reduced graphene oxide with enhanced electrocatalytic activity for ultrasensitive detection of H₂O₂. Sens Actuators B Chem. 2018;260:529–40.
- [9] Allen MJ, Tung VC, Kaner RB. Honeycomb carbon: A review of graphene. Chem Rev. 2010;110:132-45.
- [10] Dreyer DR, Park S, Bielawski CW, Ruoff RS. The chemistry of graphene oxide. Chem Soc Rev. 2010;39:228-40.
- [11] Shao Y, Wang J, Wu H, Liu J, Aksay IA, Lin Y. Graphene based electrochemical sensors and biosensors: A review. Electroanalysis. 2010;22:1027–36.
- [12] Aparicio-Martínez E, Ibarra A, Estrada-Moreno IA, Osuna V, Dominguez RB. Flexible electrochemical sensor based on laser scribed Graphene/Ag nanoparticles for non-enzymatic hydrogen peroxide detection. Sens Actuators B Chem. 2019;301:127101.
- [13] Wang R, Liu X, Zhao Y, Qin J, Xu H, Dong L, et al. Novel electrochemical non-enzymatic glucose sensor based on 3D Au@Pt core-shell nanoparticles decorated graphene oxide/multi-walled carbon nanotubes composite. Microchem J. 2022;174:107061.
- [14] Song X, Wang D, Kim M. Development of an immuno-electrochemical glass carbon electrode sensor based on graphene oxide/gold nanocomposite and antibody for the detection of patulin. Food Chem. 2021;342:128257.
- [15] Liu Y, She P, Gong J, Wu W, Xu S, Li J, et al. A novel sensor based on electrodeposited Au-Pt bimetallic nano-clusters decorated on graphene oxide (GO)-electrochemically reduced GO for sensitive detection of dopamine and uric acid. Sens Actuators B Chem. 2015;221:1542-53.
- [16] Nechaeva NL, Boginskaya IA, Ivanov AV, Sarychev AK, Kurochkin IN. Multiscale flaked silver SERS-substrate for glycated human albumin biosensing. Anal Chim Acta. 2019;1100:250-7.

- [17] De S, Higgins TM, Lyons PE, Nirmalraj PN, Blau WJ, Boland JJ, et al. Silver nanowire networks as flexible, transparent, conducting films: Extremely high DC to optical conductivity ratios. Acs Nano. 2009;3:1767–74.
- [18] Xu M, Yang F, Yuan Y, Guo Q, Ren B, Yao J, et al. Stacking faults enriched silver nanowires: Facile synthesis, catalysis and SERS investigations. J Colloid Interface Sci. 2013;407:60-6.
- [19] Wang L, Xia G, Jin L, Qi W, Chen Z, Lin X. Amperometric glucose biosensor based on silver nanowires and glucose oxidase. Sens Actuators B Chem. 2013;176:9-14.
- [20] Jiang T, Feng L, Wang Y. Effect of alginate/nano-Ag coating on microbial and physicochemical characteristics of shiitake mushroom (Lentinus edodes) during cold storage. Food Chem. 2013:141:954-60.
- [21] Kandula S, Jeevanandam P. Synthesis of Cu₂O@Ag polyhedral core-shell nanoparticles by a thermal decomposition approach for catalytic applications. Eur J Inorg Chem. 2016;10:1548–57.
- [22] Sun SD. Recent advances in hybrid Cu₂O-based heterogeneous nanostructures. Nanoscale. 2015;7:10850-82.
- [23] Faraji M, Amini M, Anbari AP. Preparation and characterization of TiO₂-nanotube/Ti plates loaded Cu₂O nanoparticles as a novel heterogeneous catalyst for the azide-alkyne cycloaddition. Catal Commun. 2016;76:72–5.
- [24] Wang G, van den Berg R, Donega CD, de Jong KP, de Jongh PE. Silica-supported Cu₂O nanoparticles with tunable size for sustainable hydrogen generation. Appl Catal B-Environ. 2016;192:199–207.
- [25] Xu H, Ye SJ, Fan Z, Ren FH, Gao CJ, Li QB, et al. Zhang, preparation of Cu_2O nanowire-blended polysulfone ultrafiltration membrane with improved stability and antimicrobial activity. J Nanopart Res. 2015;17:409.
- [26] Yang K, Yan Z, Ma L, Du Y, Peng B, Feng J. A facile one-step synthesis of cuprous oxide/silver nanocomposites as efficient electrode-modifying materials for nonenzyme hydrogen peroxide sensor. Nanomaterials. 2019;9:523.
- [27] Chen L, Guo S, Dong L, Zhang F, Gao R, Liu Y, et al. SERS effect on the presence and absence of rGO for Ag@Cu₂O core-shell. Mater Sci Semicond Process. 2019;91:290-5.
- [28] Prasad MNV, Reddy YM. Growth and characterization of Ag-Cu₂O thin films: DC magnetron sputtering method. Mater Today Proc. 2020;27:486-91.
- [29] Luo Y, Xing L, Hu C, ZhangW, Lin X, Gu J. Facile synthesis of nanocellulose-based Cu₂O/Ag heterostructure as a surfaceenhanced Raman scattering substrate for trace dye detection. Int J Biol Macromol. 2022;205:366-75.
- [30] Hu F, Song B, Wang X, Bao S, Shang S, Lv S, et al. Green rapid synthesis of Cu₂O/Ag heterojunctions exerting synergistic antibiosis. Chin Chem Lett. 2022;33:308–13.
- [31] Tang Z, He W, Wang Y, Wei Y, Yu X, Xiong J, et al. Ternary heterojunction in rGO-coated Ag/Cu₂O catalysts for boosting selective photocatalytic CO₂ reduction into CH₄. Appl Catal B Environ. 2022;311:121371.
- [32] Gan T, Wang Z, Shi Z, Zheng D, Sun J, Liu Y. Graphene oxide reinforced core-shell structured Ag@Cu₂O with tunable hierarchical morphologies and their morphology-dependent electrocatalytic properties for bio-sensing applications. Biosens Bioelectron. 2018;112:23–30.
- [33] Sharma K, Maiti K, Kim NH, Hui D, Lee JH. Green synthesis of glucose-reduced graphene oxide supported Ag-Cu₂O

- nanocomposites for the enhanced visible-light photocatalytic activity. Compos Part B Eng. 2018;138:35-44.
- [34] Wei Q, Wang Y, Qin H, Wu J, Lu Y, Chi H. Construction of rGO wrapping octahedral $Ag-Cu_2O$ heterostructure for enhanced visible light photocatalytic activity. Appl Catal B Environ. 2018;227:132-44.
- [35] Nowak A, Szade J, Talik E, ZubkoM, Wasilkowski D, Dulski M, et al. Physicochemical and antibacterial characterization of ionocity Ag/Cu powder nanoparticles. Mater Charact. 2016;117:9-16.
- [36] Rubina MS, Kamitov EE, Zubavichus YV, Peters GS, Naumkin AV, Suzeet S, et al. Collagen-chitosan scaffold

- modified with Au and Ag nanoparticles: Synthesis and structure. Appl Surf Sci. 2016;366:365-71.
- [37] Rabchinskii MK, Saveliev SD, Stolyarova DY, Brzhezinskaya M, Kirilenko DA, Baidakova MV, et al. Modulating nitrogen species via N-doping and post annealing of graphene derivatives: XPS and XAS examination. Carbon. 2021;182:593-604.
- [38] Torrisi L, Silipigni L, Cutroneo M, Torrisi A. Graphene oxide as a radiation sensitive material for XPS dosimetry. Vacuum. 2020;173:109175.
- [39] Liu S, Jiang X, Waterhouse GIN, Zhang ZM, Yu L. A Cu₂O/PEDOT/ graphene-modified electrode for the enzyme-free detection and quantification of glucose. J Electroanal Chem. 2021;897:115558.